

## RESEARCH ARTICLE

# Blocking CTGF/CCN2 reduces established skeletal muscle fibrosis in a rat model of overuse injury

Mary F. Barbe | Brendan A. Hilliard | Mamta Amin | Michele Y. Harris |  
 Lucas J. Hobson | Geneva E. Cruz | Steven N. Popoff

Department of Anatomy and Cell Biology,  
 Lewis Katz School of Medicine, Temple  
 University, Philadelphia, PA, USA

### Correspondence

Mary F. Barbe, Department of Anatomy  
 and Cell Biology, Lewis Katz School of  
 Medicine at Temple University, 3500 North  
 Broad Street, Philadelphia, PA 19140, USA.  
 Email: mary.barbe@temple.edu

### Funding information

Research reported in this publication  
 was supported by the National Institute  
 of Arthritis and Musculoskeletal and  
 Skin Diseases (NIAMS) of the National  
 Institutes of Health (NIH) under Award  
 Number AR056019. The content is solely  
 the responsibility of the authors and does  
 not necessarily represent the official views  
 of the National Institutes of Health

### Abstract

Tissue fibrosis is a hallmark of overuse musculoskeletal injuries and contributes to functional declines. We tested whether inhibition of CCN2 (cellular communication network factor 2, previously known as connective tissue growth factor, CTGF) using a specific antibody (termed FG-3019 or pamrevlumab) reduces established overuse-induced muscle fibrosis in a clinically relevant rodent model of upper extremity overuse injury. Young adult rats performed a high repetition high force (HRHF) reaching and lever-pulling task for 18 weeks, after first being shaped for 6 weeks to learn this operant task. Rats were then euthanized (HRHF-Untreated), or rested and treated for 6 weeks with FG-3019 (HRHF-Rest/FG-3019) or a human IgG as a vehicle control (HRHF-Rest/IgG). HRHF-Untreated and HRHF-Rest/IgG rats had higher muscle levels of several fibrosis-related proteins (TGF $\beta$ 1, CCN2, collagen types I and III, and FGF2), and higher muscle numbers of alpha SMA and pERK immunopositive cells, compared to control rats. Each of these fibrogenic changes was restored to control levels by the blocking of CCN2 signaling in HRHF-Rest/FG-3019 rats, as were HRHF task-induced increases in serum CCN2 and pro-collagen I intact N-terminal protein. Levels of cleaved CCN3, an antifibrotic protein, were lowered in HRHF-Untreated and HRHF-Rest/IgG rats, compared to control rats, yet elevated back to control levels in HRHF-Rest/FG-3019 rats. Significant grip strength declines observed in HRHF-Untreated and HRHF-Rest/IgG rats, were restored to control levels in HRHF-Rest/FG-3019 rats. These results are highly encouraging for use of FG-3019 for therapeutic treatment of persistent skeletal muscle fibrosis, such as those induced with chronic overuse.

### KEY WORDS

CCN2, extracellular matrix, overuse injury, TGF-beta, work-related musculoskeletal disorders

**Abbreviations:**  $\alpha$ SMA, alpha smooth muscle actin; BCA, bichinchonic acid; CD45, leukocyte common antigen; CCN1/Cyr61, cellular communication network factor 1; also known as Cysteine-rich angiogenic inducer 61; CCN2, cellular communication network factor 2; also known as connective tissue growth factor, CTGF; CCN3/NOV, cellular communication network factor 3; also known as nephroblastoma overexpressed; Fsp1, fibroblast-specific growth factor 1; FG-3019, Pamrevlumab, an anti-CCN2 agent; FGF2/bFGF, fibroblast growth factor 2/basic fibroblast growth factor; FRC, food-restricted controls; gf, grams of force; HRH, high repetition high force; IgG, immunoglobulin; pERK, phosphorylated extracellular signal-related kinase; NK1RA, neurokinin 1 receptor antagonist; PINP, pro-collagen I intact N-terminal protein; PDGFR $\beta$ , platelet-derived growth factor receptor beta; PINP, Pro-collagen I intact N-terminal protein; SMA, smooth muscle actin; TGF $\beta$ 1, transforming growth factor beta 1; vWC, von Willebrand factor type C domain.

This is an open access article under the terms of the Creative Commons Attribution-NonCommercial License, which permits use, distribution and reproduction in any medium, provided the original work is properly cited and is not used for commercial purposes.

© 2020 The Authors. *The FASEB Journal* published by Wiley Periodicals, Inc. on behalf of Federation of American Societies for Experimental Biology

## 1 | INTRODUCTION

Overuse-induced musculoskeletal disorders are widely understood to be injuries and disorders affecting the musculoskeletal system.<sup>1</sup> Tissue fibrosis is a pathological hallmark of overuse-induced muscle injuries and is considered to play key roles in associated motor dysfunction. Such fibrosis is thought to distort dynamic properties of tissue and contribute to functional declines due to adherence of adjacent structures.<sup>2-4</sup> We have shown that inflammation is a key driver of further fibrosis, and that early use of anti-inflammatory drugs, ergonomic task reduction and manual therapy treatments are able to prevent their development.<sup>5-10</sup> However, treatments aimed at reducing established muscle and other tissue fibrosis have proved to be more difficult,<sup>11-14</sup> because once deposited and cross-linked, the extracellular matrix becomes resistant to degradation.<sup>15</sup> There is even evidence from studies examining fibrotic kidneys that fibroblasts collected from these fibrotic kidneys have undergone epigenetic alterations that render these cells chronically activated.<sup>16</sup> However, blocking CCN2 (cellular communication network factor 2; previously known as connective tissue growth factor, CTGF<sup>17,18</sup>) signaling has shown promise for many fibrotic disorders,<sup>19</sup> as explained further below.

CCN2 is a secreted matricellular protein with four modular domains that independently interact with different molecules, such as collagen and proteoglycans in the extracellular matrix.<sup>20</sup> CCN1/Cyr61 (also known as Cysteine-rich angiogenic inducer 61) and CCN3/NOV (also known as nephroblastoma overexpressed) are two family members that can have similar or opposing functions in fibrogenic processes as CCN2, respectively.<sup>21-23</sup> Downregulation of CCN2 by antisense or siRNA treatment reduces liver fibrosis and limits hypertrophic scarring without affecting wound healing.<sup>24,25</sup> Mdx mice (an animal model of Duchenne muscular dystrophy) with hemizygous CCN2 deletion, or treatment with a monoclonal antibody that targets the von Willebrand factor type C (vWC) domain of CCN2, show reduced muscle fibrosis and improved locomotion and muscle strength.<sup>15,26</sup> The anti-CCN2 antibody, known as FG-3019 or pamrevlumab, inhibits mesothelioma growth and cell proliferation in three different human mesothelioma cells lines and induces apoptosis in mesothelioma cells and fibroblasts.<sup>27</sup> FG-3019 also mitigates skin fibrosis in conjunction with a reduction in the numbers of cells expressing platelet derived growth factor receptor beta (PDGFR $\beta$ ), procollagen, alpha-smooth muscle actin ( $\alpha$ SMA), pSmad2, and fibroblast-specific growth factor 1 (Fsp1) in the dermis of a preclinical mouse model of systemic sclerosis.<sup>28</sup> This agent successfully attenuated the progression of idiopathic pulmonary fibrosis in phase 2 trials<sup>29,30</sup> (NCT01262001, NCT01890265), and is currently in phase 3 development for this disorder as well as for locally advanced, unresectable pancreatic cancer<sup>31</sup> (NCT03941093). This treatment is also currently in phase 2 trials for Duchenne muscular dystrophy (NCT02606136).

We recently found that CCN2 is critical to the early progression of chronic overuse-induced muscle fibrosis and grip strength declines in rats that performed an operant reaching, grasping, and lever-pulling task at high repetition high force (HRHF) levels for three weeks.<sup>19</sup> Systemic injections of the FG-3019 agent reduced this early progression of musculotendinous fibrosis, and improved motor declines. However, continued performance of the HRHF task for 18 weeks, untreated, induces even greater muscle fibrosis and motor declines than at earlier weeks.<sup>4</sup> Therefore, we examined for the first time whether inhibition of CCN2 using this antibody is able to reduce established skeletal muscle fibrosis in our operant rat model of overuse injury.

## 2 | METHODS

### 2.1 | Overview of animals

Experiments were approved by the Temple University Institutional Animal Care and Use Committee in compliance with NIH guidelines for the humane care and use of laboratory animals. Studies were conducted on 56 young adult to mature (3 mo of age at onset of the experiments and 10.5 mo of age at completion), female, Sprague Dawley rats (Charles Rivers, Wilmington, MA). Thirty-one of these rats were randomly divided into one of four groups: (a) age-matched food restricted controls (FRC,  $n = 10$ ); (b) task rats that were shaped and then performed an HRHF task for 18 weeks (HRHF-Untreated,  $n = 10$ ); and (c,d) 18-week task rats that then rested for 6 weeks with simultaneous treatment with an anti-CCN2 antibody (HRHF-Rest/FG-3019 rats,  $n = 6$ ); or a human immunoglobulin (HRHF-Rest/IgG,  $n = 5$ , as a vehicle control) before euthanasia (Figure 1). The remaining 25 rats were used to assay serum levels of estradiol, as described further below under enzyme-linked immunosorbent assays (ELISAs).

Rats were weighed twice per week, provided regular rat chow daily in addition to food reward pellets (banana and chocolate pellets, Bio-Serv, Flemington, NJ), and allowed to gain weight over the course of the 30-week experiment.<sup>19</sup> FRC rats received similar amounts of rat chow and food reward pellets as HRHF rats. One animal in the HRHF-Rest/IgG group died from unknown reasons in task week 12 (this group was originally  $n = 6$ ; thereby reducing to final number to  $n = 5$  for this group). Further rat care details are as previously described.<sup>19</sup>

### 2.2 | HRHF task

Custom-designed operant behavioral chambers were used in which rats performed an operant reaching and lever pulling task, as previously described.<sup>32-34</sup> As an overview,

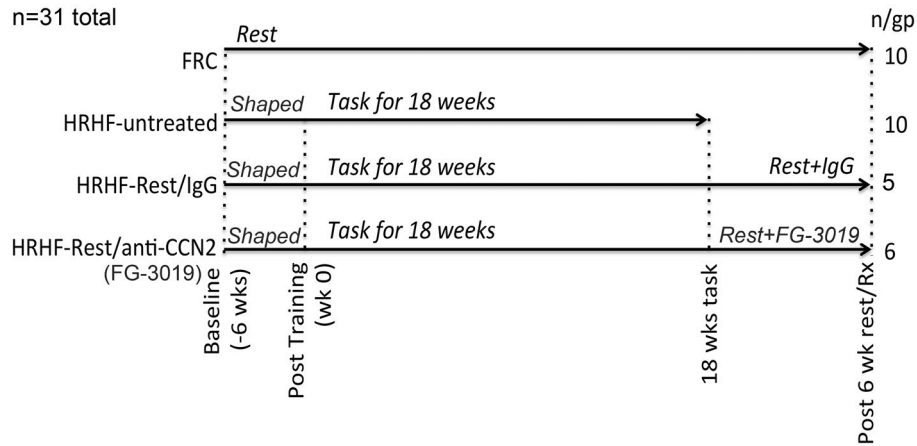


**FIGURE 1** Design of experiment. Young adult female Sprague Dawley rats were randomly divided into one of four groups: age- and weight-matched food-restricted controls (FRC); task rats that were handled for 1 wk and then shaped for 6 wk, before going on to perform a HRHF task for 18 wk (HRHF-Untreated); and task rats that performed the HRHF task for 18 wk before cessation of the task for 6 wk with simultaneous systemic treatment with a human immunoglobulin (HRHF-Rest/IgG) or with an anti-CCN2 antibody called FG-3019 or pamrevlumab (HRHF-Rest/FG-3019, hereafter), before euthanasia. Additional animals were used for serum estradiol assays, as delineated in Figure S3

task rats were shaped for 6 weeks to learn a reaching and lever-pulling task at high force loads. Rats then performed an HRHF reaching and lever-pulling task for 18 weeks for a food reward. For this, rats reached through a shoulder height portal and pulled on a vertical 1.5-mm metal bar, positioned 2.5 cm outside of the chamber wall that was attached to a load cell (Futek Advanced Sensor Technology, Irvine, CA). The load cell was interfaced with custom written Force Lever software that allowed us to choose a required force level for provision of a food reward (Med Associates, St. Albans, VT). Auditory indicators (Med Associates) cued the animal to attempt a reach every 15 seconds. Task rats had to grasp the force lever and exert an isometric pull toward the chamber wall with a graded force effort of  $48\% \pm 5\%$  of their maximum voluntary pulling force (~144 grams force (gf)). The rats' mean peak maximum pulling force was determined on the last day of shaping by requiring the rat to pull at increasing levels for a food reward until their maximum level was reached. They also had to reach and pull on the lever bar at a reach rate of 4 reaches/min, for 2 h/d, in 30-min intervals (with 1.5-h break between session), for 3 d/wk. If the animal reached and pulled on the lever bar at the correct force level and held it for at least 90 ms, within the 500-ms sound-cued period, a light signal signified that a 45-mg food pellet reward was dispensed into a trough located at floor height for the animal to lick up.

We have previously shown that the animals develop discomfort from the task and switch limbs or use both limbs simultaneously to pull on the lever bar in their attempt to garner a food reward pellet, beginning in task weeks 2 and 3.<sup>4,9,10</sup> Therefore, limbs used to reach were recorded by individuals observing the rats during each task session. Bilateral pulling of the lever bar was recorded upon occurrence, as was

incidence of a rat switching the forearm used to pull on the lever bar from their original “preferred” reach limb (determined during the shaping period) to the contralateral limb. Incidence of bilateral pulling or switching the limb used to pull the lever increased significantly across the weeks of task performance, beginning around task weeks 2-3, as previously reported.<sup>4,9,10</sup> We found that before week 18 that all of the 18-week HRHF animals utilized either forearm, or both, to pull the lever bar interchangeably across the weeks.

### 2.3 | Pharmacological treatments

The 6 HRHF-Rest/FG-3019 rats performed the HRHF task for 18 weeks, before resting for 6 weeks while being treated 2×/wk with a human anti-CCN2 monoclonal antibody (FG-3019, FibroGen, Inc, San Francisco, CA; 40 mg/kg body wt, i.p.). The FG-3019 drug was provided by the company in small amounts, in sealed glass vials, at the appropriate concentration of the projected weights of the rats at the time of the injections (weight projections were based on our prior experience with similar aged rats<sup>4,33</sup>). All rats were weighed immediately prior to injections, and the FG-3019 dose adjusted as needed to provide 40 mg/kg body wt, i.p. The five HRHF-Rest/IgG rats performed the HRHF task for 18 weeks, before resting for 6 weeks while being treated 2×/wk for 6 weeks with a human immunoglobulin (IgG; FibroGen; 50 microl/injection, i.p.) as the vehicle control. Effects of FG-3019 and IgG in control rats have been reported (no negative side effects were observed).<sup>19,35</sup>

The FG-3019 antibody used here has been previously characterized and targets domain II of CCN2, the vWC domain, located within the amino-terminal half of the full length protein.<sup>20,36</sup> This domain is thought to stimulate

collagen synthesis and bind proteoglycans in the extracellular matrix (other specific associations are being clarified).<sup>20</sup> We previously examined using western blot if FG-3019 treatment affected the ability to immunochemically detect CCN2, using tissues from control rats since CCN2 levels should be similar.<sup>19</sup> No differences in CCN2 levels were seen in tendons and serum of FRC versus FRC + FG-3019 rats.<sup>19</sup>

## 2.4 | Grip strength assays

All HRHF and control rats were assayed for reflexive grip strength. Reflexive grip strength of both forelimbs was measured individually using a 1027SR-D58, Columbus Instruments, Columbus, Ohio with a standard pull bar and sensor ranges from 0 to 5 kg to best assay rat grip strength. The test was repeated 3-5 times/limb, with peak force recorded by the manufacturer software. Grip strength is reported from assays performed the day prior to euthanasia. Mean maximum grip strength is reported per trial.

## 2.5 | Tissue collection

Animals were deeply anesthetized with 5% isoflurane in oxygen, and then euthanized by performing thoracotomy and cardiac puncture for blood collection using a 23-gauge needle. Collected blood was placed into uncoated 15-mL tubes and allowed to clot for 1 hour before being centrifuged at 12 000 rpm for 20 minutes at 4°C. Serum was harvested and frozen at -80°C until assayed. Flexor digitorum muscles were collected from the euthanized animals' mid forearm region from 10 age-matched FRC rats, 10 HRHF-Untreated rats, 6 HRHF-Rest/FG-3019 rats, and 5 HRHF-Rest/IgG rats, as shown in Figure 1. Task rats used both limbs to reach; therefore, muscles from one limb per rat were collected unfixed and tested using protein assays (the opposite limb was used for immunohistochemistry). A randomization schema was used so that a mix of right and left limbs was collected for each assay choice. For protein assays, muscles were separated from tendons and bones using a scalpel. Muscle samples were rinsed in sterile saline and flash frozen before storage at -80°C until use, at which time they were thawed on ice and homogenized in 100-mL sterile, ice-cold, phosphate-buffered saline (PBS) containing proteinase inhibitors (ThermoFisher, Waltham, MA). After centrifugation,<sup>19</sup> muscle supernatants were collected and frozen at -80°C until assayed.

After anesthesia, euthanasia and collection of serum and muscles from one limb per rat for protein assays, as described above, all rats underwent intracardial perfusion with saline and then buffered 4% paraformaldehyde. After fixation, a 2.5-mm-thick piece of flexor digitorum muscle was removed from mid- to proximal forearm for crosssectional

cryosectioning (14 µm) after cryopreservation first in 10% and then in 30% sucrose in phosphate buffer across 4 days (48 hours per sucrose solution), and then embedding in OCT (Fisher Healthcare Tissue-Plus OCT Compound Embedding medium, FisherScientific) before cryosectioning. The distal muscle-nerve mass was also removed, similarly cryopreserved, embedded in OCT, and longitudinally cryosectioned (14 µm). Sections were placed onto charged slides (Fisher Scientific, Fair Lawn, NJ), dried overnight at room temperature, before storage in foil-wrapped slide boxes at -80°C until use.

## 2.6 | ELISAs

Serum samples from 10 age-matched FRC, 10 HRHF-Untreated, 5 HRHF-Rest/IgG, and 6 HRHF-Rest/FC-3019 were batch assayed for CCN2 (USBiological, Salem, MA) and PINP (pro-collagen I intact N-terminal protein, MyBiosource, San Diego, CA). ELISAs were conducted using manufacturers' protocols, in duplicate, and reported as pg per ml of serum. Estradiol levels were also analyzed in serum using ELISA (ES180S-100, Calbiotech SKU) from 7 HRHF-Untreated and 5 HRHF-Rest/IgG (termed "Shape + Task 18 wk" and "Shape + Task 18 wk + 6 weeks rest" in Figure S3), as well as from 25 additional rats in order to examine for potential effects of shaping, task, or rest on serum estradiol levels. These 25 additional animals were constituted five groups: 5 normal control rats that were 3 months of age ("NC (-7 wk)"), 5 food-restricted only control rats that were 3.2 months of age ("FRC (-6 wk)"), 5 food-restricted animals that were shaped for 6 weeks ("Post shaping (0 wk)"), 4 food-restricted and shaped rats that performed the HRHF task for 12 weeks ("Shape + Task 12 wk"), and 6 food-restricted only rats that were shaped for 6 weeks before resting for 24 weeks ("Shape + 24 wk Rest") (Figure S3).

Muscle homogenate samples from 10 age-matched FRC, 10 HRHF-Untreated, 5 HRHF-Rest/IgG, and 6 HRHF-Rest/FC-3019 were batch assayed using ELISAs for transforming growth factor beta 1 (TGFβ1, Enzo, New York, NY), CCN2 (USBiological, Salem, MA), collagen types I and III (LSBio, Seattle, WA), and FGF2 (also called basic fibroblast growth factor, bFGF, MyBiosource). ELISAs were conducted using manufacturers' protocols, in duplicate. Data (pg of protein) were normalized to µg total protein, determined using a bicinchoninic acid (BCA) protein assay kit.

## 2.7 | Western blot analysis

Electrophoresis and western blot analysis of muscle supernatants were performed for analysis of CCN1 and CCN3 levels, using described methods.<sup>19</sup> Equal amounts of protein

were reduced, denatured, and boiled for 5 minutes at 100°C. Samples were resolved on 10% Tris-Glycine SDS gels. Gels were immunoblotted onto nitrocellulose membranes. Membranes were Ponceau S stained, then destained before blocking for 1 hour in 5% BSA in TBST and then incubating with primary antibodies. Primary antibodies against CCN1 used were: CCN1 antibody (1:1000 dilution, AF4055, R&D, Minneapolis, MN), a CCN1 antibody that recognizes mouse CCN1 (1:200 dilution, a gift from B Chaqour, SUNY Downstate Medical Center).<sup>37</sup> The antibody used to assay for CCN3 was raised in goat (1AF1976, R&D), diluted 1:1000 in Can Get Signal (Toyobo, Japan) before incubating with membranes. After washing, blots were incubated with appropriate secondary antibodies diluted 1:15 000-1:20 000 in the Can Get Signal buffer. Images were taken using a LI-COR System, and then densitometric analysis was performed using Image J. Ponceau S stained densitometric data for each individual lane was used to normalize the density of target protein signal in each individual lane after antibody staining, as previously described.<sup>19</sup> CCN1 and CCN3 gels were repeated until 5-6 different samples per group were assayed.

The specificity of the antibody used to detect CCN1 has been previously described.<sup>37</sup> A preabsorption protein blocking step was used to verify specificity of the R&D anti-CCN3 antibody used for western blotting using a recombinant CCN3 protein (1640-NV-050, R&D) at 10:1 ratio (rCCN3:antibody). Additionally, secondary antibody only incubations of membrane strips were performed for CCN1 and CCN3.

## 2.8 | Immunohistochemistry

Muscle cryosections were immunostained in batched sets by the same individual for CCN2 (sc14939, Santa Cruz Biotechnology, 1:1000 dilution in PBS), collagen type 1 (ab6308, AbCam, Cambridge, MA, 1:300 dilution in PBS), alpha smooth muscle actin ( $\alpha$ SMA, A2547, dilution 1:500, Sigma), phosphorylated extracellular signal-regulated kinase (pERK, 4370, 1:200 dilution in PBS, Cell Signaling, Danvers, MA), or with an anti-human IgG tagged with Dylight 650 (ab96906, Abcam) to detect the FG-3019 antibody, using previously described methods.<sup>4,19</sup> Sections were blocked with 5% goat serum and were then incubated with primary antibodies in moist incubation chambers overnight at room temperature. Appropriate secondary antibodies were diluted 1:100 in PBS and incubated on sections for 2 hours before washing in PBS. DAPI was used as a nuclear stain before coverslipping with 80% glycerol in PBS.

Specificity of the CCN2 and collagen type I antibodies used for immunohistochemistry was determined using western blots to check if the antibodies detected bands at the correct molecular weights. Membranes were incubated with primary antibodies overnight at 4°C. For CCN2, gels were made as

described earlier for CCN1 and 3. For collagen type I, 8% gels were made without SDS in the gel, yet with SDS in sample and loading buffers, as described.<sup>38</sup> The antibodies used detected bands at the correct molecular weights (Figure S1A,B).

Preabsorption antibody-protein blocking steps were also performed to demonstrate either the CCN2 or collagen type 1 specificity using CCN2 recombinant protein (CXT-687, Prospec, East Brunswick, NJ) and collagen type 1 rat protein (C7661, Sigma). A two- to threefold excess of purified protein, respectively, was preincubated with the matching antibody overnight at 4°C, the mixture centrifuged, and the preabsorbed antibody supernatant incubated with the tissues (after pepsin and goat serum treatment) before washing and incubation with secondary antibodies. No staining was observed in tissues after this preabsorption (Figure S1C). Specificity of the anti- $\alpha$ SMA antibody used has been previously reported.<sup>4</sup>

Antibody specificity of the anti-human IgG tagged with Dylight 650 (Abcam) was determined for the anti-human IgG by staining sections from animals not been injected with FG-3019.

## 2.8.1 | Quantification methods

Quantification of staining was performed in batched sets by individuals blinded to group assignment, using an upright microscope with both bright field and epifluorescent features (E800, Nikon, Melville, NY) that was interfaced with a digital camera (Retiga 4000R QImaging Firewire Camera, Surry, BC Canada), PC computer, and an image analysis system (Bioquant Image Analysis Corporation, Nashville, TN). In flexor digitorum muscles,  $\alpha$ SMA immunopositive cells were counted in mid to proximal regions of the flexor digitorum muscle (crosssections), in three fields per muscle and rat. Size exclusion limits were imposed with the Bioquant software so that only  $\alpha$ SMA + cells between 2 and 15  $\mu$ m in diameter were counted. The pERK antibody immunostained both small cells on the perimeter of myocytes and well as subsets of myocytes. Therefore, these different cell types were quantified separately in mid- to proximal regions of the flexor digitorum muscle (crosssections). Results are presented as the number of cells/mm<sup>2</sup>.

## 2.9 | Statistical analyses

An a priori power analysis was performed using data from our prior studies on grip strength.<sup>10,39</sup> We chose the most conservative sample size needed to detect differences with an alpha level of .05 and 80% power. This power analysis indicated the estimated sample size needed was 5 per group. Therefore, a minimum of 5 per group and per assay were

utilized. GraphPad Prism version 8.2 was used for the statistical analyses. ELISA, western blot, serum protein, cell numbers, and grip strength data were compared using one-way ANOVAs, followed by Tukey's post hoc tests. Pearson correlations were used to compare grip strength to fibrogenic protein levels, and fibrogenic protein levels to each other. Spearman's rho correlations were used to compare total reaches across the 18 weeks of task performance and CCN2 levels in serum and muscle. Significance was set at  $P = .05$  and results are reported as mean  $\pm$  SEM.

### 3 | RESULTS

#### 3.1 | Blocking CCN2 signaling reduced HRHF-induced increases of CCN2 and Collagen I immunorexpression in muscles

Since we have previously reported increased CCN2 and collagen type I in 18-week untreated HRHF rats in the endomysium around myofibers, myotendinous and scar-like regions within flexor digitorum muscles,<sup>4,8</sup> we first sought to determine if those results were replicated. HRHF-Untreated muscles contained areas with dense endomyseal deposition of CCN2 and collagen type I around myofibers (Figure 2A). These regions were found in band-like formations (indicated by an asterisk) and around myofibers (arrows) in flexor digitorum muscles examined at mid-forearm level in cross-sectional slices. We next examined the effects of systemic Rest/IgG and Rest/FG-3019 treatments. Muscles in the HRHF-Rest/IgG group (Figure 2B) looked similar to those of the HRHF-Untreated group. In contrast, blocking CCN2 signaling reduced CCN2 and collagen type I deposition around myofibers in HRHF-Rest/FG-3019 muscles, and in a similar presumed myotendinous origin in the same mid-forearm regions as examined in the first two groups (Figure 2C). FRC rat muscles in the same flexor muscle region showed little to no endomyseal CCN2 or collagen type I deposition (Figure 2D).

In order to ascertain if the FG-3019 agent reached the interior of the flexor digitorum muscle belly, we stained muscles with an anti-human IgG antibody tagged with Dylight 650 (since the FG-3019 is a human antibody). FG-3019 was detected on the perimeter of myofibers in HRHF-Rest/FG-3019 rat muscles (Figure 3A), as previously reported.<sup>19</sup> No staining was observed in untreated HRHF rat muscles (Figure 3B).

#### 3.2 | Blocking CCN2 signaling mitigated HRHF-induced increases of muscle fibrosis-related proteins

Levels of CCN2 and collagen type I, as well as several other fibrosis-related proteins, were quantified in flexor

digitorum muscles using ELISA. The HRHF-Untreated and HRHF-Rest/IgG rats had higher muscle levels of TGF $\beta$ 1, CCN2, collagen types I and III, and FGF2/bFGF, compared to FRC rat levels (Figure 4A-E). Blocking CCN2 signaling reduced levels of each protein to control rat levels in HRHF-Rest/FG-3019 rat muscles (Figure 4). HRHF-Rest/FG-3019 rats also showed significantly lower muscle levels of TGF $\beta$ 1, CCN2, and collagen type I, compared to HRHF-Untreated rats, (Figure 4A-C) and lower muscle levels of TGF $\beta$ 1, CCN2, collagen type III, and FGF2/bFGF (Figure 4A,B,D,E), compared to HRHF-Rest/IgG rats.

#### 3.3 | Blocking CCN2 signaling mitigated HRHF-induced increases of serum CCN2 and procollagen

HRHF-Untreated rats showed higher serum levels of TGF $\beta$ 1, CCN2, and PINP, compared to FRC rat levels (Figure 5A-C). Despite the 6 week rest period and treatments, HRHF-Rest/IgG and HRHF-Rest/FG-3019 rats continued to show high-serum TGF $\beta$ 1, compared to FRC rats (Figure 5A). However, the rest period lowered serum CCN2 in both groups (Figure 5B). Yet only FG-3019 treatment significantly lowered serum PINP levels in HRHF-Rest/FG-3019, compared to HRHF-Untreated rats and HRHF-Rest/IgG rats (Figure 5C).

#### 3.4 | Blocking CCN2 signaling reduced HRHF-induced increases in muscle $\alpha$ SMA and pERK immunopositive cells

Since TGF $\beta$ 1 increases in tissues are often associated with increases in  $\alpha$ SMA immunopositive (+) cells,<sup>4</sup> we examined flexor digitorum muscles for the latter. We observed increased numbers of small  $\alpha$ SMA + cells on the perimeter of myofibers in HRHF-Untreated and HRHF-Rest/IgG rat muscles, compared to FRC muscles (Figure 6A-C; since the HRHF-Rest/IgG looked similar to HRHF-Untreated animals, their data is shown only in Figure 6A). The  $\alpha$ SMA immunorexpression co-localized with CCN2 immunorexpression in these small perimeter cells (Figure 6B). Blocking CCN2 signaling significantly lowered the number of  $\alpha$ SMA + cells in HRHF-Rest/FG-3019 muscles, compared to both HRHF-Untreated and HRHF-Rest/IgG muscles (Figure 6A,D).

We also observed increased numbers of small pERK + cells on the perimeter of myofibers in HRHF-Untreated and HRHF-Rest/IgG rat muscles, compared to HRHF-Rest/FG-3019 and FRC muscles (Figure 7A-E). Blocking CCN2 signaling significantly lowered the number of small pERK + cells in

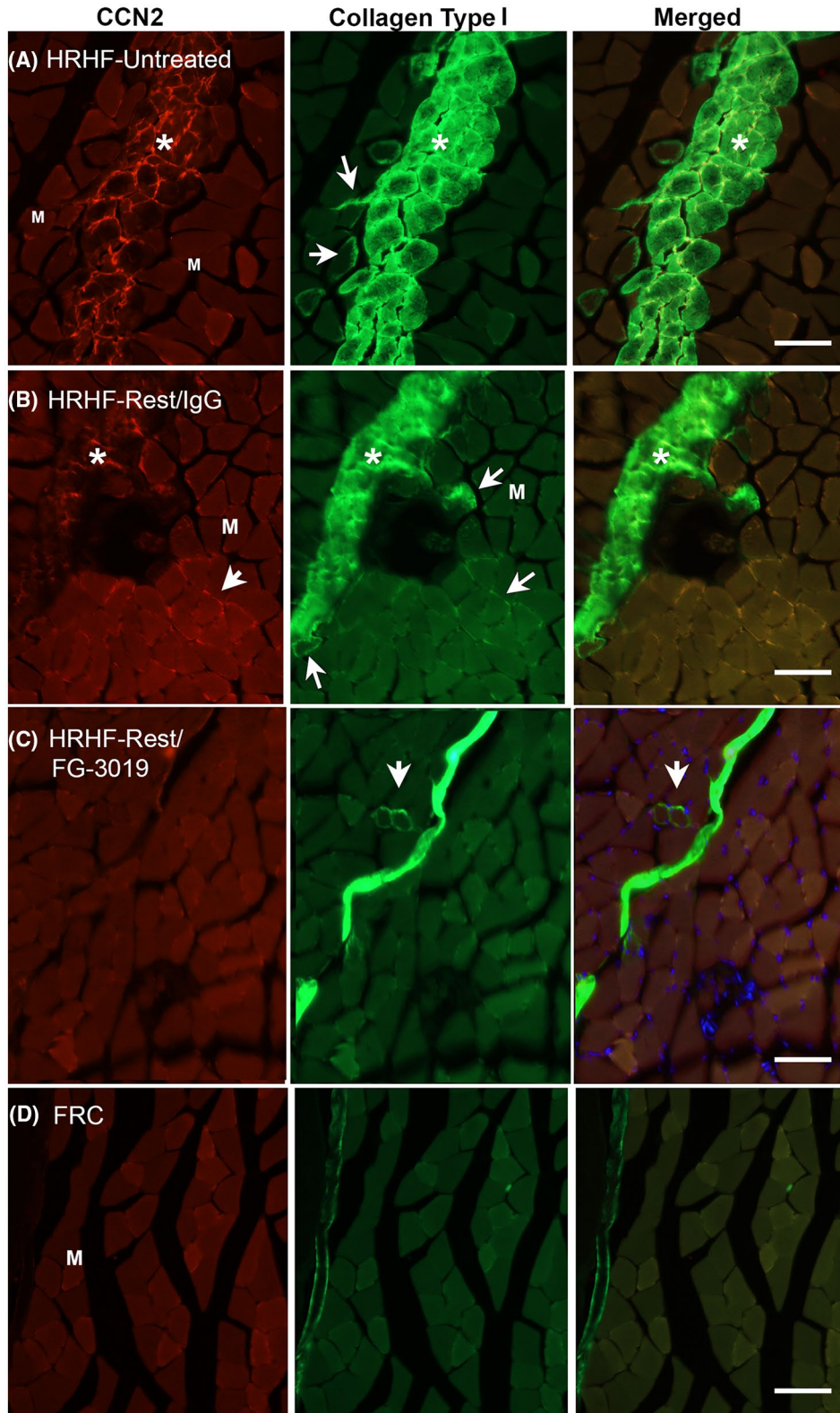
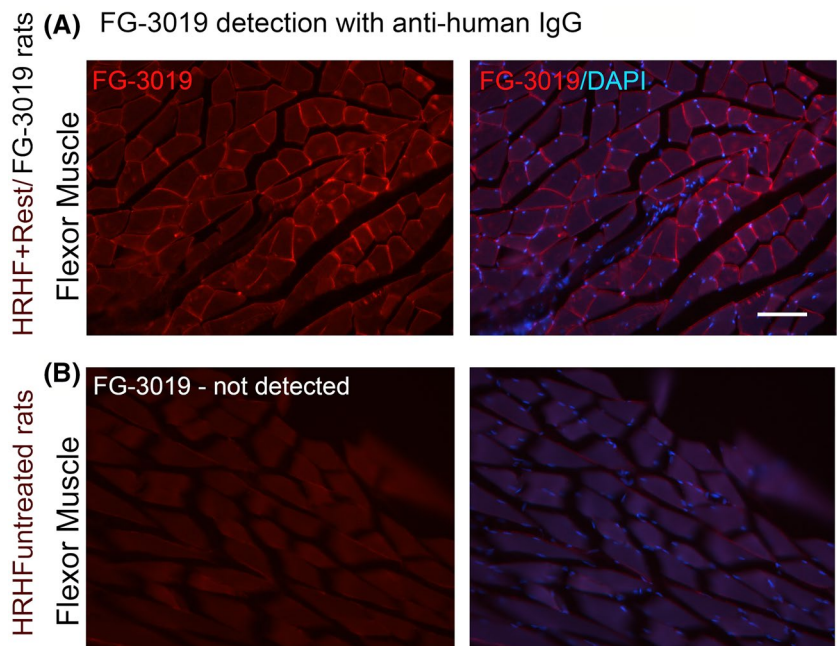


**FIGURE 2** Representative CCN2 (red) and collagen type I (green) immunoeexpression in the flexor digitorum muscles of each group. Representative images of mid-forearm cross sections are shown. A and B, HRHF-Untreated and HRHF-Rest/IgG muscles showing areas with dense endomyseal deposition of CCN2 and collagen type I around individual myofibers and in band-like formations. Asterisks indicate the band-like formations. Arrows indicate examples of myofibers surrounded by endomyseal CCN2 or collagen type I. C, HRHF-Rest/FG-3019 muscles in the same flexor muscle region showed clear reductions in CCN2 and collagen type I deposition. D, FRC rat muscles in the same flexor muscle region showed little to no endomyseal CCN2 or collagen type I deposition. M = muscle. Scale bar = 50 microns

**FIGURE 3** Anti-human IgG detection of the FG-3019 agent in flexor digitorum muscles. A, FG-3019 was detected around individual myofibers of HRHF-FG-3019 rats using an anti-human IgG antibody (red). B, This staining was not detected in HRHF-untreated rat muscles. DAPI (blue) was used as nuclear counter stain (right images of both A and B). Similar results were seen in five animals per group. Scale bar = 50 microns



HRHF-Rest/FG-3019 muscles, compared to both HRHF-Untreated and HRHF-Rest/IgG muscles (Figure 6A,D). The number of myofibers with cytoplasmic pERK immunostaining in HRHF-Untreated and HRHF-Rest/IgG rat muscles was also higher than in FRC muscles (Figure 7).

### 3.5 | Blocking CCN2 signaling rescued HRHF-induced declines in muscle CCN3

We next examined the effects of task and treatment on two other CCN family members: CCN3 (Figure 8) and CCN1 (Figure S2). The anti-CCN3 detected at ~39 kDa, ~38, and ~30 kDa (two representative blots are show in Figure 8A,B). The ~39-kDa band did not alter across groups. However, the ~38- and ~30-kDa bands were lower in HRHF-Untreated and HRHF-Rest/IgG rat muscles, relative to FRC and HRHF-Rest/FG-3019 rat muscles (Figure 4A). Densitometry confirmed these results (Figure 8C). Incubation of the anti-CCN3 antibody used with a recombinant CCN3 protein blocked all staining in western blots (Figure 8D), confirming its specificity.

### 3.6 | CCN1 levels were not altered by task or treatment

One antibody used to assay anti-CCN1 recognized a ~28-kDa form of CCN1 (Figure S2A). A second antibody used recognized ~80-Da, ~48- and ~38-kDa forms of CCN1 (Figure S2B). No task or treatment induced changes were observed (Figure S2).

### 3.7 | Blocking CCN2 signaling restored HRHF-induced declines in grip strength, which correlated with muscle levels of fibrogenic proteins

Grip strength was lower in HRHF-Untreated rats and HRHF/Rest-IgG, compared to FRC rats, and restored to FRC rat levels in HRHF-Rest/FG-3019 rats (Figure 9A). These declines had moderate to strong negative and significant associations with TGF $\beta$ 1 ( $P = .01$ ), CCN2 ( $P = .02$ ), collagen type 1 ( $P = .005$ ), collagen type III ( $P = .049$ ), and FGF2/bFGF ( $P = .048$ ) (Pearson correlation coefficient  $r$  values are shown in Figure 9B). The various fibrosis-related proteins also had strong positive and significant associations with each other ( $P < .01$  each, with  $r$  values shown in Figure 9B).

### 3.8 | Total number of reaches correlates with CCN2 levels in muscle and serum

The total number of reaches performed by all 3 groups of HRHF task rats by the end of task week 18 was  $6668 \pm 810.2$  (Mean  $\pm$  SEM). When total reach data from all three groups of rats was compared to muscle and serum levels of CCN2, no significant correlations were observed. However, when data from just the HRHF-Untreated and HRHF-Rest/IgG rats were included in the correlational statistical model, the total number of reaches performed by an individual rat ( $6324 \pm 882$ , Mean  $\pm$  SEM) correlated strongly and positively with CCN2 levels in the individual reach limb muscles used for ELISA (Spearman's  $r = .54$ ,  $P = .03$ ) and with CCN2 levels in their serum (Spearman's  $r = .074$ ,  $P = .002$ ).

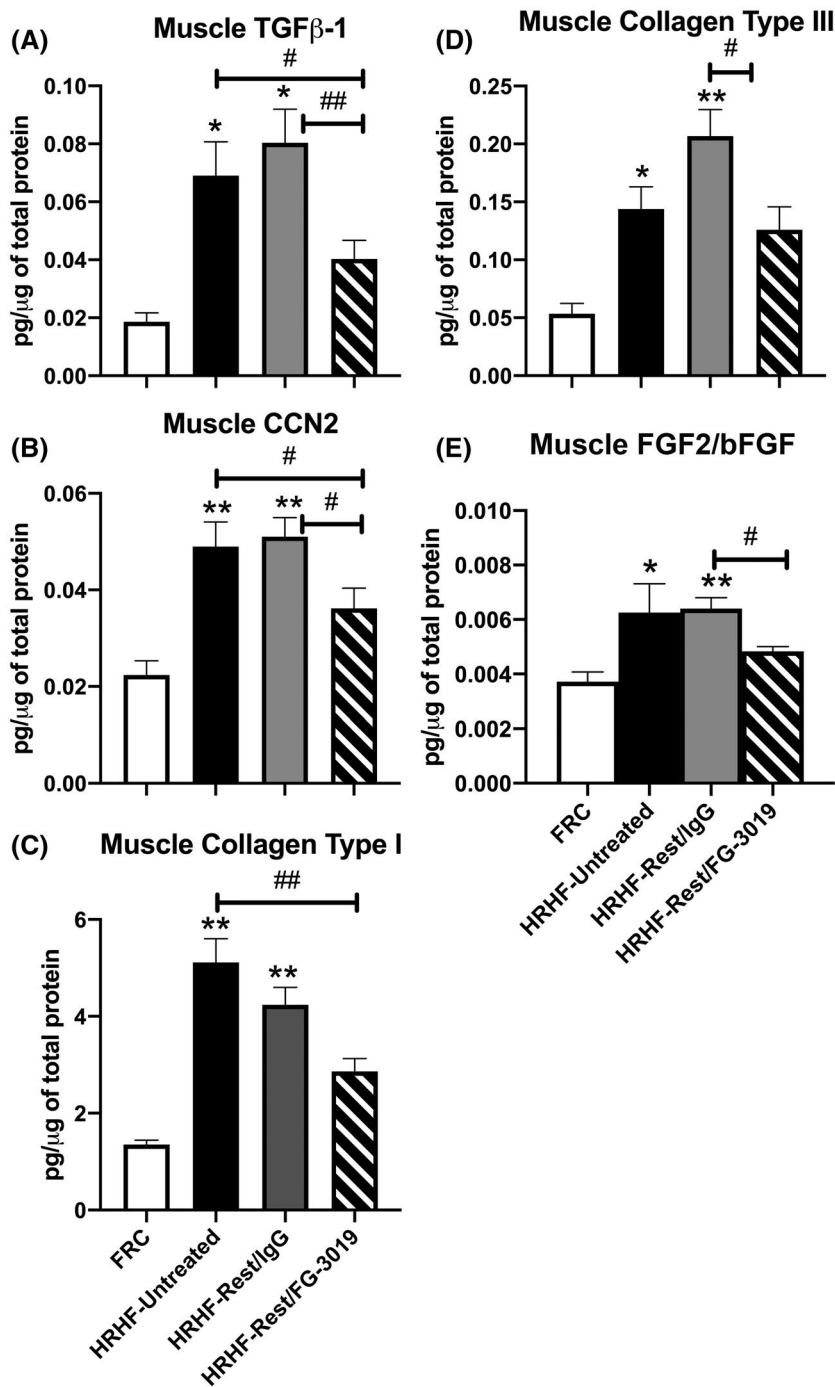


**FIGURE 4** Flexor digitorum muscle levels of fibrosis-related proteins, quantified using ELISA. A, Muscle levels of TGF $\beta$ 1 (transforming growth factor beta 1). B, Muscle levels of CCN2 (cell communication network protein 2, CTGF). C and D, Muscle levels of collagen types I and III. E, Muscle levels of FGF2/bFGF (basic fibroblast growth factor). \* $P < .05$  and \*\* $P < .01$ , compared to FRC rats; # $P < .05$  and ## $P < .01$ , compared to HRHF-Untreated or HRHF-Rest/IgG rats as shown. Number/group:  $n = 10$  FRC,  $n = 10$  HRHF,  $n = 5$  HRHF-Rest/IgG, and  $n = 6$  HRHF-Rest/FG-3019. Mean  $\pm$  SEM shown

### 3.9 | Neither Shaping, task performance, nor rest altered circulating estradiol levels

We tested estradiol levels in serum collected from several control, shaped and task groups to ascertain if the task interfered with circulating estradiol levels. No significant changes in serum estradiol levels are evident between any control (normal control and FRC) versus several shaping and task groups (immediately post-shaping which is task week 0, shaping followed by a 24-week rest, task week 12 and task week 18 groups, are included), or between HRHF-Untreated versus

HRHF-Rest/IgG-treated groups (these latter groups were renamed as “Shape + Task weeks 18” and “Shape + Task 18 + 6 weeks Rest,” respectively, for easier comparison to the other groups tested for circulating estradiol levels), as shown in Figure S3.

## 4 | DISCUSSION

We have previously reported progressive muscle fibrosis and motor declines in rats performing this same arduous high demand reaching and grasping task for 3-18 weeks.<sup>4,19</sup> We

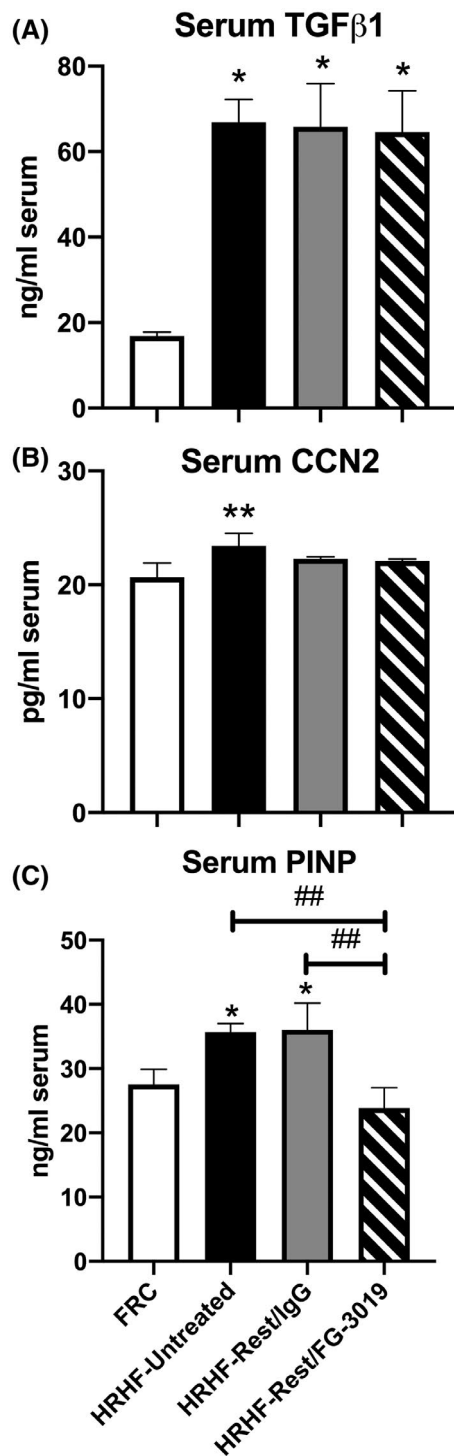


**FIGURE 5** Serum levels of fibrosis-related proteins, tested using ELISA. A, Serum levels of TGFβ1. B, Serum levels of CCN2. C, Serum levels of PINP (pro-collagen I intact N-terminal protein). \* $P < .05$  and \*\* $P < .01$ , compared to FRC rats; ## $P < .01$ , compared to HRHF-untreated or HRHF-Rest/IgG rats as shown. Number/group:  $n = 10$  FRC,  $n = 10$  HRHF,  $n = 5$  HRHF-Rest/IgG, and  $n = 6$  HRHF-Rest/FG-3019. Mean  $\pm$  SEM shown

recently reported that the early use of an anti-CCN2 drug (FG-3019) prevents the early progression of these changes.<sup>19</sup> We extended that work here to examine whether the FG-3019

agent can reverse established muscle fibrosis and motor dysfunction. We show here for the first time in an operant overuse injury model that 6 weeks of rest combined with systemic FG-3019 treatment significantly reduced established skeletal muscle fibrosis, reduced numbers of  $\alpha$ SMA immunopositive cells, and improved motor function, compared to control rat levels. We again show that increased muscle fibrosis was mirrored by increased serum levels of CCN2,<sup>4,19</sup> adding further support to its use as a serum biomarker of underlying tissue fibrosis occurring with overuse injuries as well as other diseases associated with enhanced fibrogenic activity.<sup>40,41</sup>

Past findings of tissue fibrosis after prolonged performance for 12-18 weeks of this high repetition high force, HRHF, task were replicated in this present study, including increased muscle levels of TGFβ1, CCN2, and collagen type I, as were reductions in grip strength.<sup>4,42</sup> We now also report an increase in muscle levels of FGF2/FGF and serum PINP levels in 18 week HRHF-Untreated rats. The increase in muscle FGF2/FGF is interesting because selective blocking of the FGFR1-mediated pathway with a selective FGF receptor 1 tyrosine kinase inhibitor (NP603) has been shown to decrease hepatic collagen deposition and alpha-SMA expression in an in vivo rat model of liver fibrosis.<sup>43</sup>

We also found that 6 weeks of rest with systemic human IgG treatment did not effectively reduce muscle fibrosis or improve motor function in the HRHF-Rest/IgG rats. While this may appear to be in contrast to another recent study from our lab in which rest fairly effectively reduced skeletal muscle levels of fibrogenic proteins in rats that performed a more moderate low repetition high force task for 12 weeks,<sup>39</sup> rather than the more prolonged (18 week) and higher demand (high repetition high force) task used in this present study. Yet, even with that shorter moderate task, rest failed to restore muscle hypercellularity and grip strength declines to control rat levels.<sup>39</sup> Instead, normal tissue histology and function was restored only when rest was combined with a neurokinin-1 receptor antagonist (NK1RA) that blocked Substance P signaling (a known inducer of collagen production in a variety of tissue types<sup>44</sup>). Our present results are in line with a study reporting that rest alone was ineffective in reducing collagen and other noncontractile tissue in skeletal muscles by 6 weeks of repeated chronic strain injury (50 strains daily, 5 times weekly for 6 weeks to hyperactive soleus muscles in which hyperactivity was induced by tetanus toxin).<sup>45</sup> In that study, 3 months of ambulation only (with no induced strains and cessation of tetanus induced hyperactivity) did not lower muscle levels of collagen, which remained 18% above control levels. Thus, rest alone is not enough to allow recovery from established muscle fibrogenic changes induced in chronically strained or overloaded muscles.

CCN2/CTGF has been shown to modulate many signaling pathways leading to extracellular matrix deposition.<sup>46</sup> It

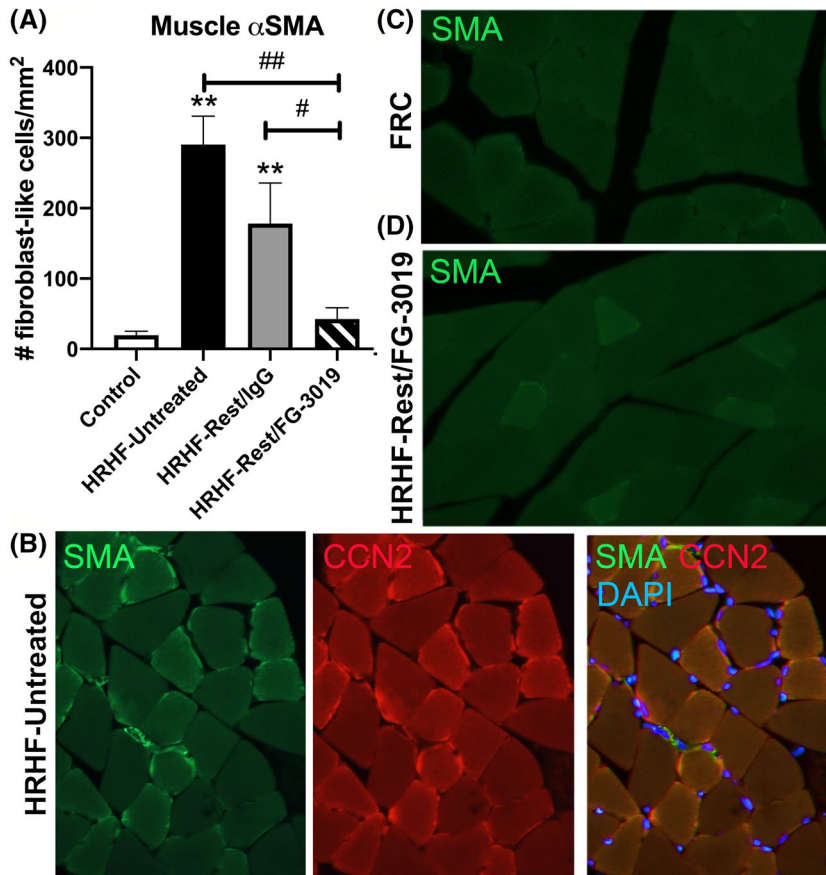


**FIGURE 6** Numbers of alpha smooth muscle actin (SMA) immunopositive stained cells in flexor digitorum muscle. Only small cells were between 2 and 15 microns in diameter were quantified. A, Quantification results for numbers of alpha SMA immunopositive cells in cross-sectionally cut flexor digitorum muscles. B and C, Representative images of alpha SMA (green) in groups as shown. Middle and right panels of B also show co-localization of SMA with CCN2 (red). Dapi (blue) was used as a nuclear counter stain. \*\* $P < .01$ , compared to FRC rats; # $P < .05$  and ## $P < .01$ , compared to HRHF-Untreated or HRHF-Rest/IgG rats as shown. Mean  $\pm$  SEM shown. Images taken with a 20 x objective

plays a key role in matrix over-production and is markedly elevated in fibrotic organs and tissues from animal models and humans with various fibrotic diseases ranging from hepatic fibrosis, renal disease with fibrosis, mesothelioma, idiopathic pulmonary fibrosis, muscle dystrophy, skin fibrosis, overuse injury, and more.<sup>24,26-29,47</sup> CCN2 is a downstream mediator of TGF $\beta$ 1,<sup>48,49</sup> and increases in tissues under conditions of overload.<sup>50</sup> Yet, in the context of this model of overuse injury, blocking CCN2 signaling also reduces TGF $\beta$ 1 production in the muscles. A study examining retinas of diabetic rats also found that inhibition of CTGF gene expression inhibited TGF $\beta$ 2.<sup>51</sup> CCN2 overexpression mediates the ensuing fibrosis with increased collagen in a mouse model of dystrophic skeletal muscle, and causes decreased muscle isometric force.<sup>26</sup> When this CCN2 overexpression was blocked, the dystrophy phenotype is reversed and muscle structure was restored with normalization of CCN2 levels.<sup>26</sup> Matching our results, use of FG-3019 in a mouse model of Duchenne muscular dystrophy reverses muscle tissue fibrosis and restores skeletal muscle function, with few side effects.<sup>15</sup> FG-3019 has also been shown to improve skeletal muscle structure and function in a murine model of amyotrophic lateral sclerosis.<sup>52</sup> In that latter study, they found that FGF-3019 not only reduced muscle fibrosis and improved locomotor function, it also reduced myelin degeneration in the sciatic nerve and appeared to

improve cell-cell communication across the neuromuscular junction.<sup>52</sup> That said, although FG-3019 has clear antifibrotic effects in several systems, the underlying molecular basis for the activity of FG-3019 remains uncertain. It is likely that antibody binding to CTGF interferes with interaction of CTGF with some of its putative binding partners. FG-3019 could also act as a clearance antibody, removing CTGF from the vicinity of the cells on which it acts. But the relative contribution of each of these mechanisms remains to be determined. In addition, by inhibiting CTGF function through one of these mechanisms, the expression of CTGF expression decreases. This effect of CTGF inhibition on CTGF expression is probably the result of attenuating feedback loops mediated by CTGF-binding partners and/or changes in matrix stiffness.”

TGF $\beta$ 1 is known to stimulate differentiation of fibroblast into  $\alpha$ SMA + myofibroblasts.<sup>53</sup> The increased alpha SMA + cells in untreated HRHF rat muscles was prevented by blocking CCN2 signaling with the FG-3019 treatment, as was pERK. FG-3019 has also been shown to attenuate irradiation-induced increases of  $\alpha$ SMA-positive myofibroblasts in lungs and other TGF $\beta$ 1-induced phenotypes,<sup>54</sup> and in animal models of skin fibrosis and peritoneal fibrosis.<sup>28,55</sup> Combined, these data support a hypothesis that blocking CCN2 signaling disrupts TGF $\beta$ 1-mediated fibrogenic responses on myofibroblasts and likely other

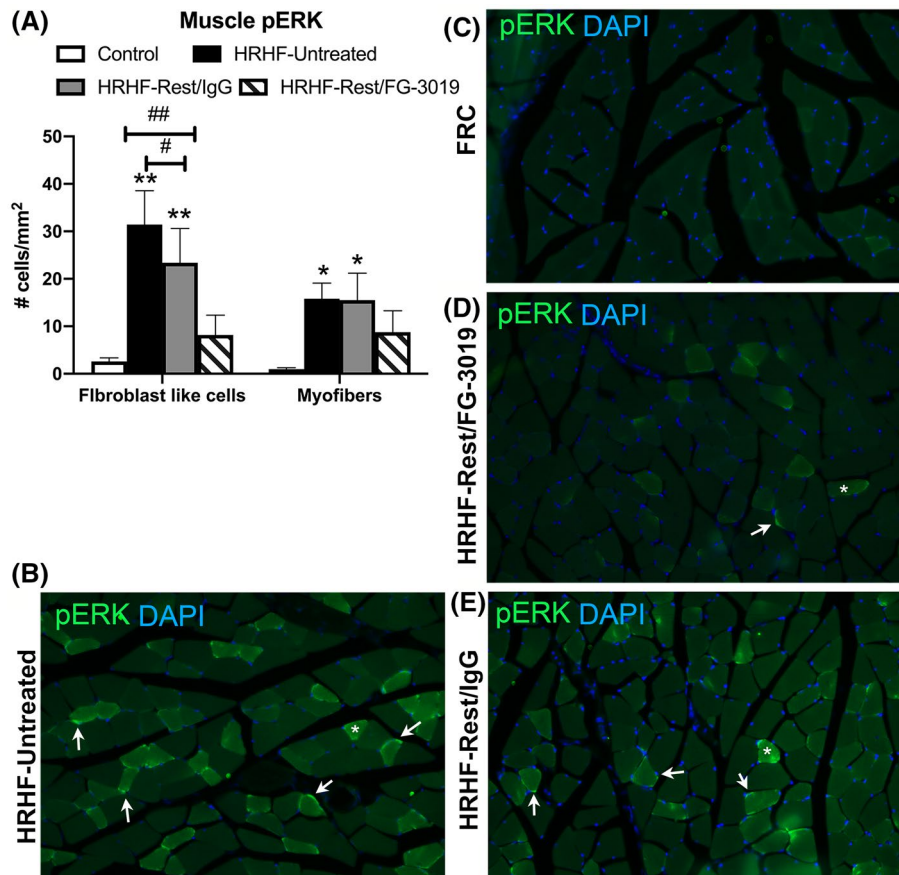


**FIGURE 7** Numbers of phosphorylated-ERK (pERK) immunopositive stained cells in flexor digitorum muscle. Both small cells between 2 and 15 microns in diameter and myofibers were quantified individually. A, Quantification results for numbers of pERK immunopositive cells in cross-sectionally cut flexor digitorum muscles. B-E, Representative images of pERK (green) in groups as shown. Dapi (blue) was used as a nuclear counter stain. Arrows indicate small fibroblastic like cells that are stained for pERK, while asterisks indicate stained myofibers. \*\* $P < .01$ , compared to FRC rats; # $P < .05$  and ## $P < .01$ , compared to HRHF-Untreated or HRHF-Rest/IgG rats as shown. Mean  $\pm$  SEM shown. Images taken with a 20 x objective

collagen-producing cells in the tissues.<sup>54</sup> Note though, as mentioned earlier, changes in FGF2, which was also lowered by FG-3019 treatment, may also be contributing to the lowered alpha SMA + cell numbers. Activation of the ERK signaling pathway has been shown as critical for modulating profibrogenic phenotype responses by liver myofibroblasts.<sup>56</sup> In vitro elevation of pERK levels is typically quite transient in response to activation, yet pERK levels were high in the 18-week HRHF-Untreated rats (in which tissues were not collected until 36 hours after the last task period) and remained high even after the 6-week rest period in the HRHF-Rest/IgG rats. The persistent increases in TGF $\beta$ 1, FGF2, and CCN2 may be the cause of persistent increase in pERK in the muscles of HRHF-Untreated and HRHF-Rest/IgG animals, similar to the earlier mentioned myofibroblasts/fibroblasts collected from these fibrotic kidneys that have become chronically activated.<sup>16,56</sup>

Regarding CCN3/NOV, two variants of CCN3 (~38 and ~30 kDa) were reduced in the HRHF-untreated and HRHF-Rest/IgG-treated animals, compared to control and

HRHF-Rest/FG-3019-treated animals. These bands are similar in molecular weights to previously identified truncated forms of CCN3 at ~38, ~32, and ~28 kDa.<sup>57-59</sup> Truncated forms of CCN3 are thought to be the biological active elements of this protein.<sup>58,60</sup> In mechanically strained fibroblasts, CCN3 levels are low during mechanical stress and increase again after relaxation.<sup>23</sup> Interestingly, CCN3 has antifibrogenic roles and antagonizes the fibrogenic effects of CCN2.<sup>21,22</sup> Perhaps its inverse expression pattern from CCN2 and increase with the FG-3019 treatment is one mechanism through which the FG-3019 agent is reducing muscle fibrosis. Since provision of CCN3 or derived peptides has been shown as a viable anti-fibrotic treatment for renal, skin, and other organ fibrosis,<sup>22,61</sup> it is possible they could remedy skeletal muscle fibrosis. Future studies are needed to examine this possibility.

We also examined flexor digitorum muscles for CCN1 levels. One anti-CCN1 antibody used in western blot assays recognized a previously identified truncated form of CCN1 at ~28 kDa,<sup>62,63</sup> while the other anti-CCN1 antibody

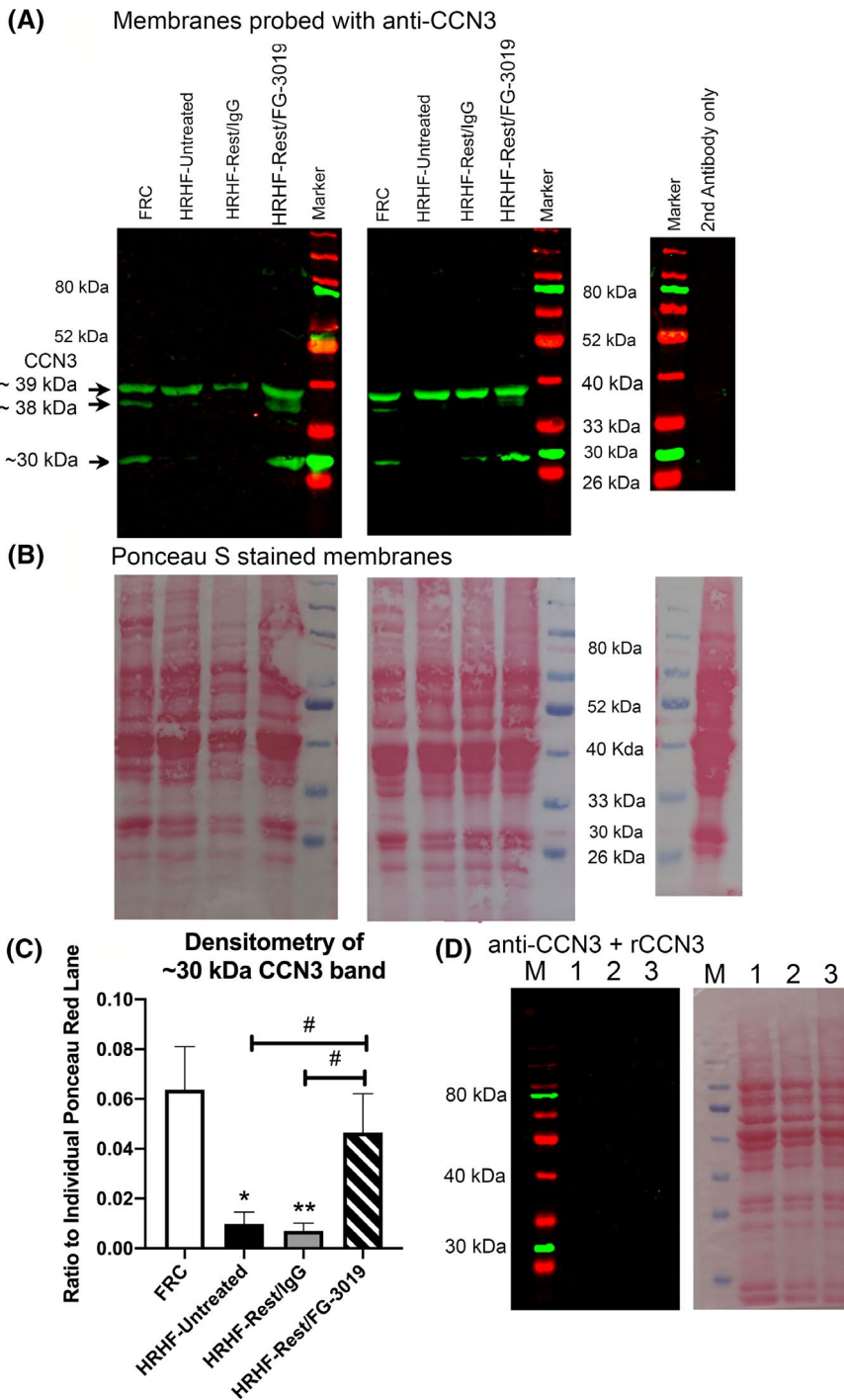


**FIGURE 8** Anti-CCN3 probed western blots. A, Left panels show two different representative western blots after probing flexor digitorum muscles with an anti-CCN3. Bands were detected at ~39 kDa; ~38 and ~30 kDa. The ~39-kDa band did not alter across groups. However, the ~38- and ~30-kDa bands were lower in HRHF-Untreated and HRHF-Rest/IgG rat muscles relative to FRC and HRHF-Rest/FG-3019 rat muscles. The far right blot shows a membrane probed with the secondary antibody only. B, Ponceau S staining of the same membranes as shown in panel A. C, Densitometry results in which CCN3 bands were compared to the total protein loaded per lane, determined from Ponceau S-stained membranes ( $n = 5-6/\text{gp}$ ). D, A preabsorption protein blocking step was used to verify specificity of the R&D anti-CCN3 antibody used for western blotting using a recombinant (r) CCN3 protein. The marker lane is indicated with an M, and lanes 1-3 are different FRC flexor digitorum muscle samples. Ponceau S staining of this same membrane is shown on the right. \* $P < .05$  and \*\* $P < .01$ , compared to FRC rats; # $P < .05$ , compared to HRHF-Untreated or HRHF-Rest/IgG rats as shown. CCN3 gels were repeated until 5-6 different samples per group were assayed. Mean  $\pm$  SEM shown in panel C

used recognized previously identified ~48- and ~38-kDa forms of CCN1.<sup>64,65</sup> That same latter antibody also recognized an ~80-kDa form of CCN1 that has not been previously reported. Perhaps the ~80-kDa band is a nonspecific band recognized by the antibody, although full knowledge of CCN1 variants is hindered as many past studies report only cropped Western blot images. Nevertheless, no changes were observed in CCN1, matching findings from a recent 3-week study from our lab.<sup>19</sup> CCN1 protein levels increase rapidly and transiently (within hours) after mechanical loading.<sup>63,66</sup> In our studies, we waited 36 hours after the last task session

to collect tissues from the 18-week HRHF-Untreated rats to avoid acute activity-induced changes in cytokines,<sup>67</sup> or 6 weeks in the task + intervention groups. As a consequence, it is possible we missed any acute changes in CCN1 levels. Thus, limitations include our inability to examine for rapid signaling changes in this chronic in vivo model, such as transient CCN1 changes.

The US Food and Drug Administration (FDA) recently granted orphan drug designation for FG-3019/pamrevlumab for the treatment of Duchenne muscular dystrophy patients. This agent is in clinical trials as a potential treatment for

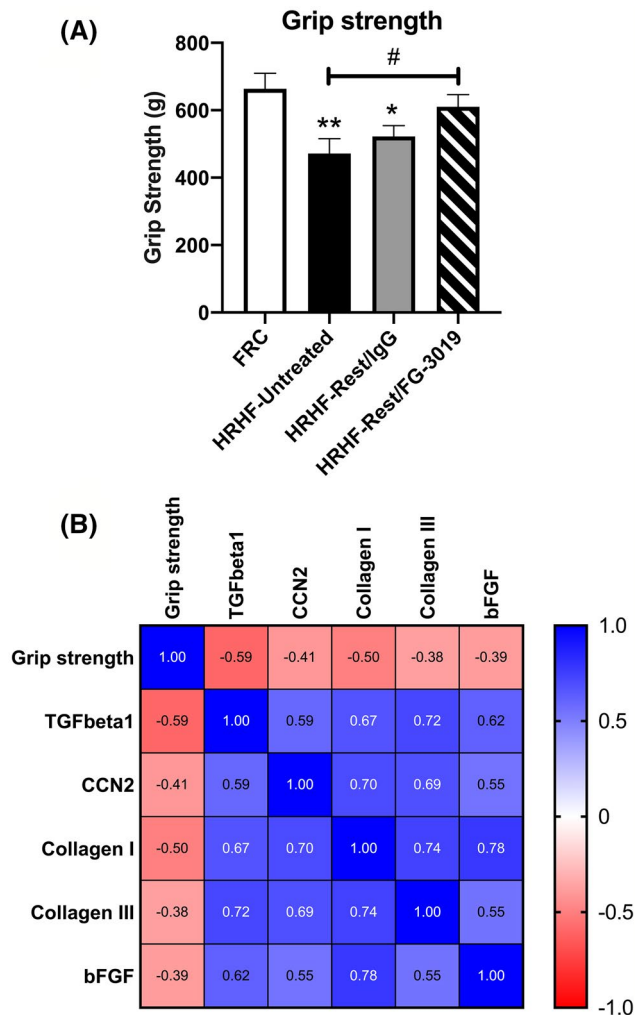


**FIGURE 9** Forearm grip strength and correlations between grip strength and fibrosis-related protein levels in flexor digitorum muscles. A, Grip strength in grams in 10 FRC rats at 30 wk after onset of experiments, 10 HRHF-Untreated rats at 24 wk after onset of experiment (ie, after 6 wk of shaping and weeks of HRHF task performance), and 5 HRHF/Rest-IgG and 6 HRHF-Rest/FG-3019 at 30 wk after onset of experiments (ie, after shaping, task, and then rest plus treatments). \* $P < .05$  and \*\* $P < .01$ , compared to FRC rats; # $P < .05$ , compared to HRHF-untreated rats. Mean  $\pm$  SEM shown. B, Correlational matrix showing Pearson correlation coefficient  $r$  values for grip strength versus ELISA-quantified levels of fibrosis-related proteins (all moderate to strong negative associations, with 0.3-0.49 interpreted as moderate, and 0.5-1 interpreted as strong) and between the different fibrosis-related proteins (all strong positive associations)

idiopathic pulmonary fibrosis and pancreatic cancer, and as it has proven beneficial and appears to be well tolerated,<sup>68</sup> it has been placed on fast track development by the FDA for these fibrotic disorders. The results of this present study provides proof of principle in a relevant operant rat model of overuse injuries that blocking CCN2 signaling using FG-3019/pamrevlumab for 6 weeks also reverses overuse-injury induced muscle fibrosis. A key strength of our model is that it is a chronic (rather than acute) operant model in which

rats develop changes in the same manner as humans involved in prolonged repetitive and forceful tasks.<sup>69</sup> We observed decreased muscle levels of TGF $\beta$ 1, FGF2, and CCN2 (each of which drive the production of collagen and other extracellular matrix proteins in a number of cell types), lowered numbers of alpha SMA and pERK immunopositive cells, and increased muscle levels of CCN3 (an antifibrogenic protein). Since CCN2 modulates a number of signaling pathways, perhaps blocking its signaling alters these downstream pathways that when combined allows normal regenerative processes to occur, resulting in restoration of muscle structure and function. Thus, these results support the feasibility of conducting clinical trials in human patients with overuse-induced fibrosis causing significant declines in muscle function.

## ACKNOWLEDGMENTS

The FG-3019 monoclonal antibody was provided by FibroGen, Inc.

## CONFLICT OF INTEREST

The authors have no financial conflicts of interest.

## AUTHOR CONTRIBUTIONS

M.F. Barbe and S.N. Popoff designed the study; M.F. Barbe, M. Amin, M.Y. Harris, and G.E. Cruz analyzed the data; M.F. Barbe, B.A. Hilliard, and S.N. Popoff wrote the paper; all authors performed the research.

## REFERENCES

1. NIOSH. National Manufacturing Agenda—June 2010. 2011. <http://www.cdc.gov/niosh/nora/comment/agendas/manuf/>.
2. Driscoll M, Blyum L. The presence of physiological stress shielding in the degenerative cycle of musculoskeletal disorders. *J Bodyw Mov Ther.* 2011;15:335-342.
3. Zugel M, Maganaris CN, Wilke J, et al. Fascial tissue research in sports medicine: from molecules to tissue adaptation, injury and diagnostics: consensus statement. *Br J Sports Med.* 2018;52:1497. <https://doi.org/10.1136/bjsports-2018-099308>.
4. Fisher PW, Zhao Y, Rico MC, et al. Increased CCN2, substance P and tissue fibrosis are associated with sensorimotor declines in a rat model of repetitive overuse injury. *J Cell Commun Signal.* 2015;1-18.
5. Jain NX, Barr-Gillespie AE, Clark BD, et al. Bone loss from high repetitive high force loading is prevented by ibuprofen treatment. *J Musculoskelet Neuronal Interact.* 2014;14:78-94.
6. Rani S, Barbe MF, Barr AE, Litvin J. Role of TNF alpha and PLF in bone remodeling in a rat model of repetitive reaching and grasping. *J Cell Physiol.* 2010;225:152-167.
7. Kietrys DM, Barr AE, Barbe MF. Exposure to repetitive tasks induces motor changes related to skill acquisition and inflammation in rats. *J Mot Behav.* 2011;43:465-476.
8. Abdelmagid SM, Barr AE, Rico M, et al. Performance of repetitive tasks induces decreased grip strength and increased fibrogenic proteins in skeletal muscle: role of force and inflammation. *PLoS ONE.* 2012;7:e38359.

9. Bove GM, Delany SP, Hobson L, et al. Manual therapy prevents onset of nociceptor activity, sensorimotor dysfunction, and neural fibrosis induced by a volitional repetitive task. *Pain*. 2019;160:632-644.
10. Bove GM, Harris MY, Zhao H, Barbe MF. Manual therapy as an effective treatment for fibrosis in a rat model of upper extremity overuse injury. *J Neurol Sci*. 2016;361:168-180.
11. Stauber WT, Knack KK, Miller GR, Grimmatt JG. Fibrosis and intercellular collagen connections from four weeks of muscle strains. *Muscle Nerve*. 1996;19:423-430.
12. Klinkhammer BM, Goldschmeding R, Floege J, Boor P. Treatment of renal fibrosis—turning challenges into opportunities. *Adv Chronic Kidney Dis*. 2017;24:117-129.
13. Mann CJ, Perdiguero E, Kharraz Y, et al. Aberrant repair and fibrosis development in skeletal muscle. *Skelet Muscle*. 2011;1:21.
14. Mahdy MAA. Skeletal muscle fibrosis: an overview. *Cell Tissue Res*. 2019;375:575-588.
15. Morales MG, Gutierrez J, Cabello-Verrugio C, et al. Reducing CTGF/CCN2 slows down mdx muscle dystrophy and improves cell therapy. *Hum Mol Genet*. 2013;22:4938-4951.
16. Bechtel W, McGoohan S, Zeisberg EM, et al. Methylation determines fibroblast activation and fibrogenesis in the kidney. *Nat Med*. 2010;16:544-550.
17. Perbal B, Tweedie S, Bruford E. The official unified nomenclature adopted by the HGNC calls for the use of the acronyms, CCN1-6, and discontinuation in the use of CYR61, CTGF, NOV and WISP 1–3 respectively. *J Cell Commun Signal*. 2018;12:625-629.
18. Perbal B, Tweedie S, Bruford E. Correction to: The official unified nomenclature adopted by the HGNC calls for the use of the acronyms, CCN1-6, and discontinuation in the use of CYR61, CTGF, NOV and WISP 1–3 respectively. *J Cell Commun Signal*. 2019;13:435.
19. Barbe MF, Hilliard BA, Delany SP, et al. Blocking CCN2 reduces progression of sensorimotor declines and fibrosis in a rat model of chronic repetitive overuse. *J Orthop Res*. 2019;37:2004-2018.
20. Kaasboll OJ, Gadicherla AK, Wang JH, et al. Connective tissue growth factor (CCN2) is a matricellular preproprotein controlled by proteolytic activation. *J Biol Chem*. 2018;293:17953-17970.
21. Riser BL, Najmabadi F, Perbal B, et al. CCN3 (NOV) is a negative regulator of CCN2 (CTGF) and a novel endogenous inhibitor of the fibrotic pathway in an in vitro model of renal disease. *Am J Pathol*. 2009;174:1725-1734.
22. Leask A. Yin and Yang revisited: CCN3 as an anti-fibrotic therapeutic? *J Cell Commun Signal*. 2015;9:97-98.
23. Schild C, Trueb B. Three members of the connective tissue growth factor family CCN are differentially regulated by mechanical stress. *Biochim Biophys Acta*. 2004;1691:33-40.
24. George J, Tsutsumi M. siRNA-mediated knockdown of connective tissue growth factor prevents N-nitrosodimethylamine-induced hepatic fibrosis in rats. *Gene Ther*. 2007;14:790-803.
25. Sisco M, Kryger ZB, O'Shaughnessy KD, et al. Antisense inhibition of connective tissue growth factor (CTGF/CCN2) mRNA limits hypertrophic scarring without affecting wound healing in vivo. *Wound Repair Regen*. 2008;16:661-673.
26. Morales MG, Cabello-Verrugio C, Santander C, Cabrera D, Goldschmeding R, Brandan E. CTGF/CCN-2 over-expression can directly induce features of skeletal muscle dystrophy. *J Pathol*. 2011;225:490-501.
27. Ohara Y, Chew SH, Misawa N, et al. Connective tissue growth factor-specific monoclonal antibody inhibits growth of malignant mesothelioma in an orthotopic mouse model. *Oncotarget*. 2018;9:18494-18509.
28. Makino K, Makino T, Stawski L, Lipson KE, Leask A, Trojanowska M. Anti-connective tissue growth factor (CTGF/CCN2) monoclonal antibody attenuates skin fibrosis in mice models of systemic sclerosis. *Arthritis Res Ther*. 2017;19:134.
29. Richeldi L, Fernández Pérez ER, Costabel U, et al. Pamrevlumab, an anti-connective tissue growth factor therapy, for idiopathic pulmonary fibrosis (PRAISE): a phase 2, randomised, double-blind, placebo-controlled trial. *Lancet Respir Med*. 2020;8(1):25-33.
30. Wells AU. Pamrevlumab in idiopathic pulmonary fibrosis. *Lancet Respir Med*. 2020;8(1):2-3.
31. Picozzi VJ, Pipas JM, Koong AC, et al. FG-3019, a human monoclonal antibody to connective tissue growth factor, combined with chemotherapy in patients with locally advanced or metastatic pancreatic ductal adenocarcinoma. *J Cancer Clin Trials*. 2017;2:1.
32. Barbe MF, Gallagher S, Popoff SN. Serum biomarkers as predictors of stage of work-related musculoskeletal disorders. *J Am Acad Orthop Surg*. 2013;21:644-646.
33. Barbe MF, Massicotte VS, Assari S, et al. Prolonged high force high repetition pulling induces osteocyte apoptosis and trabecular bone loss in distal radius, while low force high repetition pulling induces bone anabolism. *Bone*. 2018;110:267-283.
34. Xin DL, Hadrevi J, Elliott ME, et al. Effectiveness of conservative interventions for sickness and pain behaviors induced by a high repetition high force upper extremity task. *BMC Neurosci*. 2017;18:36.
35. Brenner MC, Krzyzanski W, Chou JZ, et al. FG-3019, a human monoclonal antibody recognizing connective tissue growth factor, is subject to target-mediated drug disposition. *Pharm Res*. 2016;33:1833-1849.
36. Wang Q, Usinger W, Nichols B, et al. Cooperative interaction of CTGF and TGF-beta in animal models of fibrotic disease. *Fibrogenesis Tissue Repair*. 2011;4:4.
37. Tamura I, Rosenbloom J, Macarak E, Chaqour B. Regulation of Cyr61 gene expression by mechanical stretch through multiple signaling pathways. *Am J Physiol*. 2001;281:C1524-C1532.
38. Iannarone VJ, Cruz GE, Hilliard BA, Barbe MF. The answer depends on the question: optimal conditions for western blot characterization of muscle collagen type I depends on desired isoform. *J Biol Methods*. 2019;6:e117.
39. Barbe MF, White AR, Hilliard BA, et al. Comparing effects of rest with or without a NK1RA on fibrosis and sensorimotor declines induced by a voluntary moderate demand task. *J Musculoskelet Neuronal Interact*. 2019;19:396.
40. Zoheiry MM, Hasan SA, El-Ahwany E, et al. Serum markers of epithelial mesenchymal transition as predictors of HCV-induced liver fibrosis, cirrhosis and hepatocellular carcinoma. *Electron Physician*. 2015;7:1626-1637.
41. Sato S, Nagaoka T, Hasegawa M, et al. Serum levels of connective tissue growth factor are elevated in patients with systemic sclerosis: association with extent of skin sclerosis and severity of pulmonary fibrosis. *J Rheumatol*. 2000;27:149-154.
42. Clark BD, Al Shatti TA, Barr AE, Amin M, Barbe MF. Performance of a high-repetition, high-force task induces carpal tunnel syndrome in rats. *J Orthop Sports Phys Ther*. 2004;34:244-253.
43. Lin N, Chen S, Pan W, Xu L, Hu K, Xu R. NP603, a novel and potent inhibitor of FGFR1 tyrosine kinase, inhibits hepatic stellate cell proliferation and ameliorates hepatic fibrosis in rats. *Am J Physiol*. 2011;301:C469-C477.

44. Peng L, Agogo GO, Guo J, Yan M. Substance P and fibrotic diseases. *Neuropeptides*. 2019;76:101941.
45. Stauber WT, Smith CA, Miller GR, Stauber FD. Recovery from 6 weeks of repeated strain injury to rat soleus muscles. *Muscle Nerve*. 2000;23:1819-1825.
46. Lipson KE, Wong C, Teng Y, Spong S. CTGF is a central mediator of tissue remodeling and fibrosis and its inhibition can reverse the process of fibrosis. *Fibrogenesis Tissue Repair*. 2012;5(Suppl 1):S24.
47. Frara N, Fisher PW, Zhao Y, et al. Substance P increases CCN2 dependent on TGF-beta yet Collagen Type I via TGF-beta1 dependent and independent pathways in tenocytes. *Connect Tissue Res*. 2018;59:30-44.
48. Ito Y, Goldschmeding R, Kasuga H, et al. Expression patterns of connective tissue growth factor and of TGF-beta isoforms during glomerular injury recapitulate glomerulogenesis. *Am J Physiol Renal Physiol*. 2010;299:F545-F558.
49. Song JJ, Aswad R, Kanaan RA, et al. Connective tissue growth factor (CTGF) acts as a downstream mediator of TGF-beta1 to induce mesenchymal cell condensation. *J Cell Physiol*. 2007;210:398-410.
50. Nakama LH, King KB, Abrahamsson S, Rempel DM. VEGF, VEGFR-1, and CTGF cell densities in tendon are increased with cyclical loading: an in vivo tendinopathy model. *J Orthop Res*. 2006;24:393-400.
51. Yang H, Huang Y, Chen X, et al. The role of CTGF in the diabetic rat retina and its relationship with VEGF and TGF-beta(2), elucidated by treatment with CTGFsiRNA. *Acta Ophthalmol*. 2010;88:652-659.
52. Gonzalez D, Rebolledo DL, Correa LM, et al. The inhibition of CTGF/CCN2 activity improves muscle and locomotor function in a murine ALS model. *Hum Mol Genet*. 2018;27:2913-2926.
53. Zhao Z, Sun Y, Yang S, Cui Q, Li Z. FAK activity is required for HGF to suppress TGF-beta1-induced cellular proliferation. *Vitro Cell Dev Biol Anim*. 2015;51:941-949.
54. Bickelhaupt S, Erbel C, Timke C, et al. Effects of CTGF blockade on attenuation and reversal of radiation-induced pulmonary fibrosis. *J Natl Cancer Inst*. 2017;109:djw339.
55. Sakai N, Nakamura M, Lipson KE, et al. Inhibition of CTGF ameliorates peritoneal fibrosis through suppression of fibroblast and myofibroblast accumulation and angiogenesis. *Sci Rep*. 2017;7:5392.
56. Foglia B, Cannito S, Bocca C, Parola M, Novo E. ERK pathway in activated, myofibroblast-like, hepatic stellate cells: a critical signaling crossroad sustaining liver fibrosis. *Int J Mol Sci*. 2019;20:2700.
57. Kyurkchiev S, Yeger H, Bleau AM, Perbal B. Potential cellular conformations of the CCN3(NOV) protein. *Cell Commun Signal*. 2004;2:9.
58. Perbal B. NOV (nephroblastoma overexpressed) and the CCN family of genes: structural and functional issues. *Mol Pathol*. 2001;54:57-79.
59. Su BY, Cai WQ, Zhang CG, Martinez V, Lombet A, Perbal B. The expression of ccn3 (nov) RNA and protein in the rat central nervous system is developmentally regulated. *Mol Pathol*. 2001;54:184-191.
60. Brigstock DR. The connective tissue growth factor/cysteine-rich 61/nephroblastoma overexpressed (CCN) family. *Endocr Rev*. 1999;20:189-206.
61. Riser BL, Barnes JL, Varani J. Balanced regulation of the CCN family of matricellular proteins: a novel approach to the prevention and treatment of fibrosis and cancer. *J Cell Commun Signal*. 2015;9:327-339.
62. Choi J, Lin A, Shrier E, Lau LF, Grant MB, Chaqour B. Degradome products of the matricellular protein CCN1 as modulators of pathological angiogenesis in the retina. *J Biol Chem*. 2013;288:23075-23089.
63. Pendurthi UR, Tran TT, Post M, Rao LV. Proteolysis of CCN1 by plasmin: functional implications. *Cancer Res*. 2005;65:9705-9711.
64. Bartel F, Balschun K, Gradhand E, Strauss HG, Dittmer J, Hauptmann S. Inverse expression of cystein-rich 61 (Cyr61/CCN1) and connective tissue growth factor (CTGF/CCN2) in borderline tumors and carcinomas of the ovary. *Int J Gynecol Pathol*. 2012;31:405-415.
65. Zhang F, Hao F, An D, et al. The matricellular protein Cyr61 is a key mediator of platelet-derived growth factor-induced cell migration. *J Biol Chem*. 2015;290:8232-8242.
66. Kivela R, Kyrolainen H, Selanne H, Komi PV, Kainulainen H, Vihko V. (2007) A single bout of exercise with high mechanical loading induces the expression of Cyr61/CCN1 and CTGF/CCN2 in human skeletal muscle. *J Appl Physiol*. 1985;103:1395-1401.
67. Pedersen BK, Steensberg A, Fischer C, Keller C, Ostrowski K, Schjerling P. Exercise and cytokines with particular focus on muscle-derived IL-6. *Exerc Immunol Rev*. 2001;7:18-31.
68. Richeldi L, Fernández Pérez ER, Costabel U, et al. Pamrevlumab, an anti-connective tissue growth factor therapy, for idiopathic pulmonary fibrosis (PRAISE): a phase 2, randomised, double-blind, placebo-controlled trial. *Lancet Respir Med*. 2020;8:25-33.
69. Barr AE, Barbe MF. Pathophysiological tissue changes associated with repetitive movement: a review of the evidence. *Phys Ther*. 2002;82:173-187.

## SUPPORTING INFORMATION

Additional Supporting Information may be found online in the Supporting Information section.

**How to cite this article:** Barbe MF, Hilliard BA, Amin M, et al. Blocking CTGF/CCN2 reduces established skeletal muscle fibrosis in a rat model of overuse injury. *The FASEB Journal*. 2020;34:6554–6569. <https://doi.org/10.1096/fj.202000240RR>